

Proposal of a Sizing Algorithm for an Optimal Design of DC/DC Converters Used in Photovoltaic Conversion

Mohamed Amrouayache

Department of Electrical Engineering, Skikda University, Algeria.

Article Info

Article history:

Received May 19, 2022

Revised Jul 19, 2022

Accepted Jul 30, 2022

Keyword:

MPPT
DC/DC Converter
Closed loop
Dominating poles
Second order system

ABSTRACT

The solar energy is converted to electrical energy by means of semiconductor materials called solar panels. However, the conversion efficiency is low, and hence the need to harvest the maximum power to optimize the photovoltaic conversion, for that the MPPT (Maximum Power Point Tracker) technique is used to maximize the power delivered by the solar panel (PV); this power is very fluctuating because it depends on the lightning and the temperature, the maximum power point is acquired by a DC/DC converter connected to the closed loop MPPT algorithm. The design of the circuit (the closed loop) must be robust in the face of changes in operating points caused by variations in meteorological conditions (temperature and lighting) and must always maintain certain performances such as stability, a fast and well-damped transient system, precision. In this paper, we presented a study of closed loop, for that, we established the average small signal model of the different topologies of the converters (boost; buck, buck-boost) to have a linear model. A comparative study between the three topologies has been established, to make an optimal choice of the circuit parameters.

Copyright © 2022 Institute of Advanced Engineering and Science.
All rights reserved.

Corresponding Author:

Mohamed Amrouayache,
Department of Electrical Engineering,
Skikda University,
BP 26. El Hadaiek Road- 21000, Skikda, Algeria.
Email: amarouayachemohamed@yahoo.fr.

1. INTRODUCTION

The solar panel is used as a renewable source of energy by transforming photon energy from sunlight into electrical energy. Under a given level of illumination (G), the solar panel develops a continuous electrical current (DC), the characteristic current-tension is non-linear and is influenced by temperature. To maximize the power delivered by the solar panel (PV), a DC/DC converter controlled by a search algorithm named MPPT (Maximum power point tracker) is placed at the output of this source (PV), so that, this system operates in feedback. Figure 1.[1].

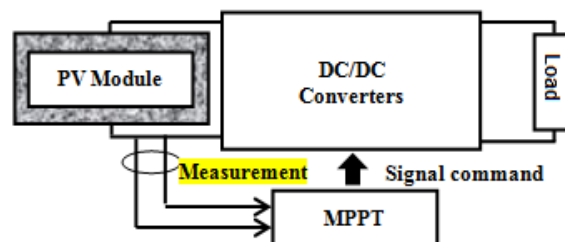


Figure 1. Block diagram of photovoltaic chain.

The search for the maximum power point is permanent (all the time), consequently the feedback system (PV, converter and MPPT) must react to each change to ensure maximum power; knowing that during a day the illumination and the temperature are variable and fluctuating, therefore the feedback quoted above often undergoes transient dynamic regimes.[2, 3]

The problem posed in solar applications is the continuous and sometimes random variation of the operating points of the circuit; so, to keep the desired performance of the system, it is necessary to choose the appropriate values and for this a dynamic study of systems (in the feedback or in open loop) is necessary to ensure certain performances such as stability, precision, rising time, overshooting. These performances are based on the different elements of the circuit studied (resistance, capacitance, inductance, measurement gain...);and even the use of a PI corrector to improve the dynamic response of the systems requires a dimensioning based on the elements of the circuit of the converter. Therefore a good choice and dimensioning of the elements of the circuit give us a robust system which remains efficient whatever the disturbances and the extreme conditions of operation [4]. In the literature, some scientific work addresses the subject of the dynamics of the *DC/DC* converter and MPPT parameters, in the works of Femia [4, 5], he proposes an improvement and optimization of the dynamic operation of MPPT and the *DC/DC* converter by a judicious choice of the sampling interval, but he gives no indication and explanation on the choice and the calculation of the parameters of the circuit, in [6] the authors presents a study of the photovoltaic chain with two stages (continuous and alternative) for robust design of the circuit against the variations of the photovoltaic source (lighting and temperature) and the side networks (imbalance of the network), and it treats the case of the continuous mode (CCM) and discontinuous mode (DCM) , but it does not give satisfactory answers on the optimization of the dynamics of the circuit during the various changes and on what the values of the capacitances and the inductances of the circuit give always transient diet best; the paper of Razman [7], he proposes a model to improve the operation of a solar emulator with the MPPT regulator, he proposes the use of a PI corrector, whose calculation of these parameters (proportional gain and integrator gain) is based on the circuit parameters (capacitance and inductance), but no indication of the capacity of the values chosen to keep the system reliable against different variations and disturbances. Among other things, in [8], and in the context of improving the continuous bus (DC-link) of a photovoltaic conversion chain, the author proposes a digital PI based on fuzzy logic, but the development presented, asks several questions regarding the choice of a second order linear system during closed loop modelling. In most of the articles cited above, the modeling is developed with the small signal modeling technique; we always end up with a linear second-order system whose dynamic study seems simple and usual; as for the photovoltaic use, we often place an input capacitor which gives us a third order system [9, 10], and in this case the dynamic study of the system becomes complex, moreover, the implementation of a PI corrector, it is not always obvious and on a large power scale it becomes very expensive. For these reasons we propose a new approach to dimension the *DC/DC* converters for photovoltaic use by a priori choice of the various elements of the circuit which gives us a powerful dynamic system whatever the variations of the operating conditions.

In this paper, we approximated the dynamic behavior of the system by a small average modeling signal in order to have a linear model, this linear model allowed us to pass to the domain of Laplace and to have the transfer functions in open loop and in closed loop. In this context, a detailed study has been established for the three topologies of *DC/DC* converters (buck, boost and buck-boost). The transfer functions obtained are third order systems, to facilitate the study of the dynamic behavior; we will introduce the concept of the dominant pole by a predefined placement of a real pole to have a second order system which will allow us to parameterize our system in relation to the desired performances.

The procedures mentioned above are summarized in an algorithm which can be programmed with simulation software; our results are presented and discussed to compare the dynamic behavior of different *DC/DC* converters used in photovoltaic applications, and determine the advantages and the disadvantages of each topology.

2. SMALL SIGNAL MODELING.

To analyze, design and control, a power electronics structure (in our case the *DC/DC* converter), we use modeling and dynamic simulation methods. Among these methods the small-signal modeling is the most widely used; this method gives us the possibility to model a nonlinear circuit with linear equations around an operating point. An equivalent circuit in which nonlinear circuit elements are replaced by linear elements whose values are given by the first-order approximation of their characteristic curve near the operating point (Often called tangential model) [11, 12]. Before starting the modeling of *DC/DC* converters, it should be noted that the operation of these converters is similar to a *DC/DC* transformer, whose transformation ratio (M) is variable, this transformation ration depends on the duty cycle (d) generated by the PWM command (pulse width modulation). Figure 2 .

The calculation of the transformation ratio, which gives a maximum operating point (The voltage that gives a maximum power V_{pv-max} and the current that gives a maximum power I_{pv-max}) requires the calculation of the maximum duty cycle. The different known MPPT algorithms, calculates the maximum operating point by calculating the maximum duty cycle (d_{max}).

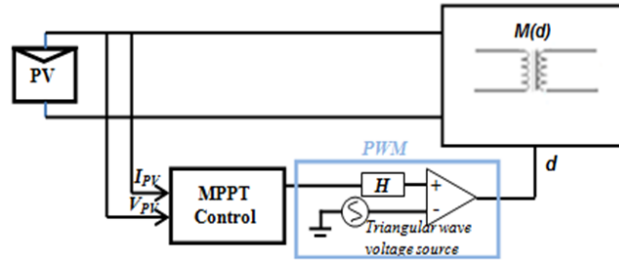


Figure 2. Model of the DC transformer with a variable transformation ratio controlled by a PWM.

The different topologies of *DC/DC* converters mainly used in photovoltaic applications are presented in table 1. L is an inductor to have a perfect direct current. C_{in} is a capacitor to filter voltage ripples at the input. C_o is a capacitor to filter voltage ripples at the output. We note that the passive components (C_{in} ; C_o ; L) is assumed to be ideal and sized away to have a continuous conduction mode (CCM) [13, 14], [15]; the transistor , and the diode are also assumed to be ideal swithes, the input voltage V_{in} is solar panel voltage V_{PV} , V_o is the output voltage.

Table 1. Topologies of different converters.

Topologies	Converter circuit	Circuit configuration while the transistor is on	Circuit configuration while the transistor is off
Buck			
Boost			
Buck-Boost			

The circuit of the converters quoted in table 1 varies in time, we have two time intervals, the first when the transistor is closed or on, and the diode is blocked ($0 \leq t \leq T_{on}$) and the second when the transistor is open or off and the diode is on ($T_{on} \leq t \leq T$); the configuration of the circuit is specified by the state of conduction and blocking of the semiconductor elements (transistor and diode), so each configuration is controlled by differential equations. The non linear time varying characteristics of switching obstructs the analysis of dynamic behaviour of converters. The linearized model has an advantage that it is time invariant around an operating point. Our small signal model in operating point characterized by two parameters , the first is the resistance ($R_{PV} = V_{PV}/I_{PV}$), which defines the operating point concerned by the small signal linearization (the maximum power point), however, the $I_{pv}(V_{PV})$ characteristic of the solar panel is nonlinear,

and the calculation of the resistance R_{PV} requires iterative numerical methods, for a better modeling of the $I_{PV}(V_{PV})$ characteristic, a new PV modeling use the *Lambertw* equation whose current I_{PV} can be expressed as a function of V_{PV} in an explicit way. The reader can find details in [15]. The second parameter is the duty cycle (d) which represents the MPPT actions.

We specify in the development which follows, that all the values of the circuit are superpositions of a continuous component (or equilibrium point) and an oscillating component that varies with time. Starting by establishing the differential equations that govern the three circuits shown in table 1 in the form of the state space model:

$$\frac{\partial x(t)}{\partial t} = A \cdot x(t) + B \cdot u(t) \tag{1}$$

And the output vector is:

$$y(t) = C \cdot x(t) \tag{2}$$

Where the tension V_{PV} , and the inductor current I_L , and the output tension V_o are the state variables.

So the state vector $x = \begin{pmatrix} V_{PV} \\ I_L \\ V_o \end{pmatrix}$; and the output vector is V_{PV} .

A is the state matrix sized (3x3); B is the control matrix sized (3x1); C is the output matrix.

$U(t) = d(t)$, is the control vector sized (1x1). In case of disturbance, we can write:

$$x(t) = X + \hat{x}(t) \quad u(t) = U + \hat{u}(t) \quad y(t) = Y + \hat{y}(t)$$

The capital values represent the equilibrium point or the continuous component, lower case letters represent the small variations around an equilibrium point or the non-continuous component which depends on time, and the hat variations ($\hat{}$) represent small variations (oscillations) around an operating point.

We substitute in equations (1) and (2) and Neglecting second order nonlinear quantities we obtain desired small signal linear state equation given by: [16, 17].

$$\hat{\dot{x}} = \bar{A} \cdot \hat{x}(t) + \bar{B} \cdot \hat{u}(t) + \hat{d}(t). [(A_1 - A_2) \cdot X + (B_1 - B_2) \cdot U] \tag{3}$$

Where:

$$\bar{A} = d \cdot A_1 + (1 - d) \cdot A_2 \tag{4}$$

$$\bar{B} = d \cdot B_1 + (1 - d) \cdot B_2 \tag{5}$$

We can have the matrices A_1, A_2, B_1, B_2 by the separate state model for each conduction and blocking interval of the semiconductor elements; so for each topology of the *DC/DC* converters the system of equations is:

For the buck topology:

$0 \leq t \leq T_{on}$	$T_{on} \leq t \leq T$
$\frac{\partial V_{PV}(t)}{\partial t} = -\frac{V_{PV}(t)}{C_{in}R_{PV}} - \frac{I_L(t)}{C_{in}}$ $\frac{\partial I_L(t)}{\partial t} = \frac{V_{PV}(t)}{L} - \frac{V(t)_o}{L}$ $\frac{\partial V_o(t)}{\partial t} = \frac{1}{C_o} I_L(t) - \frac{V_o(t)}{C_o R_o}$	$\frac{\partial V_{PV}(t)}{\partial t} = -\frac{V_{PV}(t)}{C_{in}R_{PV}}$ $\frac{\partial I_L(t)}{\partial t} = -\frac{V_o(t)}{L}$ $\frac{\partial V_o(t)}{\partial t} = \frac{1}{C_o} I_L(t) - \frac{V_o(t)}{C_o R_o}$

For the boost topology:

$0 \leq t \leq T_{on}$	$T_{on} \leq t \leq T$
$\frac{\partial V_{PV}(t)}{\partial t} = -\frac{V_{PV}(t)}{C_{in}R_{PV}} - \frac{I_L(t)}{C_{in}}$	$\frac{\partial V_{PV}(t)}{\partial t} = -\frac{V_{PV}(t)}{C_{in}R_{PV}} - \frac{I_L(t)}{C_{in}}$
$\frac{\partial I_L(t)}{\partial t} = \frac{V_{PV}(t)}{L}$	$\frac{\partial I_L(t)}{\partial t} = \frac{V_{PV}(t)}{L} - \frac{V_o(t)}{L}$
$\frac{\partial V_o(t)}{\partial t} = -\frac{V_o(t)}{C_o R_o}$	$\frac{\partial V_o(t)}{\partial t} = \frac{1}{C_o} I_L(t) - \frac{V_o(t)}{C_o R_o}$

(7)

For the buck-boost topology:

$0 \leq t \leq T_{on}$	$T_{on} \leq t \leq T$
$\frac{\partial V_{PV}(t)}{\partial t} = -\frac{V_{PV}(t)}{C_{in}R_{PV}} - \frac{I_L(t)}{C_{in}}$	$\frac{\partial V_{PV}(t)}{\partial t} = -\frac{V_{PV}(t)}{C_{in}R_{PV}} - \frac{I_L(t)}{C_{in}}$
$\frac{\partial I_L(t)}{\partial t} = \frac{V_{PV}(t)}{L} - \frac{V_o(t)}{L}$	$\frac{\partial I_L(t)}{\partial t} = -\frac{V_o(t)}{L}$
$\frac{\partial V_o(t)}{\partial t} = \frac{1}{C_o} I_L(t) - \frac{V_o(t)}{C_o R_o}$	$\frac{\partial V_o(t)}{\partial t} = \frac{1}{C_o} I_L(t) - \frac{V_o(t)}{C_o R_o}$

(8)

R_o is a resistance which characterizes the load; it can be expressed as a function of R_{PV} and the duty cycle d , according to the topology of the converter, therefore:

Using the buck topology:

$$R_o = R_{PV} \cdot d^2 \quad (9)$$

Using the boost topology:

$$R_o = R_{PV} / (1 - d)^2 \quad (10)$$

Using the buck-boost topology:

$$R_o = R_{PV} \cdot \frac{d^2}{(1-d)^2} \quad (11)$$

We substitute the equation (4),(5),(6),(7),(8),(9),(10),(11) in equation (3); we can obtain the average small signal model in matrix form as the following:

For the buck topology:

$$\frac{d}{dt} \begin{bmatrix} \hat{v}_{PV} \\ \hat{i}_L \\ \hat{v}_o \end{bmatrix} = \begin{bmatrix} -1/R_{PV}C_{in} & -1/C_{in} & 0 \\ 1/L & 0 & -(1-d)/L \\ 0 & (1-d)/C_o & -1/R_o C_o \end{bmatrix} \begin{bmatrix} \hat{V}_{PV} \\ \hat{I}_L \\ \hat{V}_o \end{bmatrix} + \begin{bmatrix} 0 \\ V_{PV} \\ -V_{PV} \\ R_{PV}C_o \end{bmatrix} \cdot \hat{d} \quad (12)$$

For the boost topology:

$$\frac{d}{dt} \begin{bmatrix} \hat{v}_{PV} \\ \hat{i}_L \\ \hat{v}_o \end{bmatrix} = \begin{bmatrix} -1/R_{PV}C_{in} & -d/C_{in} & 0 \\ d/L & 0 & -1/L \\ 0 & 1/C_o & -1/R_o C_o \end{bmatrix} \begin{bmatrix} \hat{V}_{PV} \\ \hat{I}_L \\ \hat{V}_o \end{bmatrix} + \begin{bmatrix} V_{PV} \\ d.R_{PV}C_{in} \\ V_{PV} \\ L \\ 0 \end{bmatrix} \cdot \hat{d} \quad (13)$$

For the buck-boost topology:

$$\frac{d}{dt} \begin{bmatrix} \hat{v}_{PV} \\ \hat{i}_L \\ \hat{v}_o \end{bmatrix} = \begin{bmatrix} -1/R_{PV}C_{in} & -d/C_{PV} & 0 \\ d/L & 0 & -(1-d)/L \\ 0 & (1-d)/C_o & -1/R_o C_o \end{bmatrix} \begin{bmatrix} \hat{V}_{PV} \\ \hat{I}_L \\ \hat{V}_o \end{bmatrix} + \begin{bmatrix} V_{PV} \\ d.R_{PV}C_{in} \\ V_{PV}(1-2d) \\ L(1-d) \\ V_{PV} \\ d.R_{PV}C_o \end{bmatrix} \cdot \hat{d} \quad (14)$$

For the three topologies the output equation (2) become in the average small signal model as following:

$$\hat{y}(t) = C \cdot \hat{x}(t) \quad (15)$$

$C = [1 \ 0 \ 0]$: is the output matrix.

3. TRANSFER FUNCTIONS.

After having the linear model, we can go on to the Laplace domain and model our system by a transfer function where the input is the duty cycle (\hat{d}); and the output is the tension of solar panel (\hat{V}_{PV}). Figure 3.

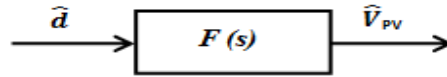


Figure 3. Transfer function (input duty cycle, output solar panel tension).

3.1. Open loop transfer function.

According to control theory of linear systems, the transfer function ($\frac{V_{PV}(s)}{d(s)}$) in the Laplace domain is defined by:

$$\frac{V_{PV}(s)}{d(s)} = C \cdot (S \cdot I - A)^{-1} \cdot B \quad (16)$$

I : is the unitary matrix.

$(S \cdot I - A)^{-1}$: is the inverse matrix of $(S \cdot I - A)$.

S : is a Laplace variable.

A, B, C : are the matrices obtained by the linear average small signal model in the equations (12), (13),(14),(15). Referring to equation (16), the transfer functions for the three topologies of DC/DC converters are in the linear form following:

For the buck topology:

$$F(s) = \frac{\left[\frac{-V_{PV}}{d \cdot R_{PV} C_{in}} \right] \cdot s^2 + \left[\frac{-V_{PV}}{d^3 \cdot C_{in} C_o R_{PV}^2} + \frac{d \cdot V_{PV}}{L C_{in}} \right] \cdot s + \left[\frac{-V_{PV}}{d \cdot L C_{in} C_o R_{PV}} \right]}{s^3 + \left[\frac{1}{R_{PV}} \left(\frac{(1-d)^2}{C_o} + \frac{1}{C_{in}} \right) \right] \cdot s^2 + \left[\frac{1}{C_o C_{in} (d \cdot R_{PV})^2} + \frac{d^2}{L C_{in}} \right] \cdot s + \frac{1}{d^2 L C_{in} C_o R_{PV}}} \quad (17)$$

For the boost topology:

$$F(s) = \frac{\left[\frac{-V_{PV}}{L C_{in} (1-d)} \right] \cdot s + \left[\frac{-2 V_{PV} \cdot (1-d)}{L C_{in} C_o R_{PV}} \right]}{s^3 + \left[\frac{1}{R_{PV}} \left(\frac{(1-d)^2}{C_o} + \frac{1}{C_{in}} \right) \right] \cdot s^2 + \left[\frac{(1-d)^2}{C_o} \left(\frac{1}{C_{in} R_{PV}^2} + \frac{1}{L} \right) + \frac{1}{L C_{in}} \right] \cdot s + \frac{2(1-d)^2}{L C_{in} C_o R_{PV}}} \quad (18)$$

For the buck boost topology:

$$F(s) = \frac{\left[\frac{-V_{PV}}{d \cdot R_{PV} C_{in}} \right] \cdot s^2 - V_{PV} \left[\frac{(1-d)^2}{d^3 \cdot C_{in} C_o R_{PV}^2} + \frac{d(1-2d)}{L C_{in} (1-d)} \right] \cdot s + \left[\frac{-V_{PV} d(1-d)}{L C_{in} C_o R_{PV}} \right]}{s^3 + \left[\frac{1}{R_{PV}} \left(\frac{(1-d)^2}{C_o} + \frac{1}{C_{in}} \right) \right] \cdot s^2 + \left[\frac{(1-d)^2}{C_o C_{in} (d \cdot R_{PV})^2} + \frac{d^2}{L C_{in}} + \frac{1}{L C_o} \right] \cdot s + \left[\frac{(1-d)^2}{L C_{in} C_o R_{PV}} \right]} \quad (19)$$

The transfer functions obtained are third order systems in the general form of a fraction as follows:

$$\frac{N(s)}{D(s)} = \frac{N_2 \cdot s^2 + N_1 \cdot s + N_0}{s^3 + D_2 \cdot s^2 + D_1 \cdot s + D_0} \quad (20)$$

The coefficients (N_2, N_1, N_0) of the nominator $N(s)$, and the coefficients (D_2, D_1, D_0) of denominator $D(s)$, characterizes the transfer function. The roots of the denominator are called the poles and these values decide the stability and the different performances of the system dynamics, the roots of the nominator are called the zeros, and they do not have a great influence on the response of the system except that they delay the response of the system. In the following paragraphs, our study and development will be concentrated on the placement of these poles and zeros to have a desired response.

3.2. The dominant poles of the second-order system.

In the study of systems, often we factor the transfer functions in the form of a product of the first order and second order subsystems, such as the following form:

$$F(s) = \frac{\prod_{i=0}^{n-1} (1+a_i.s) \prod (1+b_i.s+c_i.s^2)}{\prod_{i=0}^n (1+d_i.s) \prod (1+e_i.s+f_i.s^2)} \tag{21}$$

This decomposition into simple elements beforehand, allows us to have the response of the system as a sum or superposition of several simple first order and second order systems. The transfer functions developed before are of the third order, so we can write it in the form:

$$F(s) = \frac{N(s)}{D(s)} = \frac{N_r}{s-s_r} + \frac{N'_1.s+N'_0}{s^2+2\xi\omega_0.s+\omega_0^2} \tag{22}$$

N_r and N'_1, N'_0 are the new coefficients of the denominator of (20) after decomposition, ξ and ω_0 are the damping factor and natural pulsation of a second order system. s_r is the reel third pole of equation (20). The transfer function (20) accepts three poles, we have assigned the real pole to the first order system, and the complex poles to the second order system. For this the theory of third degree polynomials shows that the nature of the poles is decided by the value of the discriminator ($\Delta_{D(s)}$), [18].

$$\Delta_{D(s)} = (D_1D_2)^2 + 18D_2D_1D_0 - 27D_0^2 - 4D_1^3 - 4D_0D_2^3 \tag{23}$$

Hence:

- $\Delta_{D(s)} > 0$ The equation $D(s)$ admits three distinct real roots.
- $\Delta_{D(s)} = 0$ The equation $D(s)$ admits a double or triple roots and all roots are reals.
- $\Delta_{D(s)} < 0$ The equation $D(s)$ admits three distinct roots, including one reel and two conjugate complexes.

Therefore, to reduce the study of our third order system to a second order system, we must make a placement of poles such that:

$$\begin{cases} \Delta_{D(s)} < 0 \\ \text{and} \\ s_r \gg \xi\omega_0 \end{cases} \tag{24}$$

The pair of complex conjugate poles of second order is:

$$s_{1,2} = -\xi\omega_0 \mp j\omega_0\sqrt{1-\xi^2} \quad ; \text{ Where } (0 < \xi < 1) \tag{25}$$

The equation (24) introduces the notion of dominant poles, so during our design of the circuit, we place the real pole as far as possible from the imaginary axis and we place the two conjugate complex poles as close as possible to the imaginary axis. Figure 4.

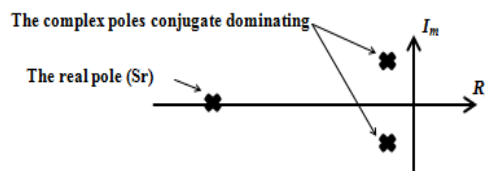


Figure 4. Location of dominant poles of a second order system.

Consequently, for having a second order system dominant by judicious pole placement, the conditions described in the system of equation (26) must be imposed:

$$\begin{cases} (s - s_r). (s^2 + 2\xi\omega_0s + \omega_0^2) = 0 \\ 0 < \xi < 1 \\ s_r \gg \xi\omega_0 \end{cases} \tag{26}$$

The solution of the system of equations (26) gives the parameters of a second order dominant system (ξ, ω_0) according to the coefficients (d_2, d_1, d_0):

$$\begin{cases} s_r = -d_2 \\ \omega_0 = \sqrt{\frac{d_0}{d_2}} \\ \xi = \frac{d_1 d_2 - d_0}{2d_2 \sqrt{d_0 d_2}} \end{cases} \quad (27)$$

Solved (27), we can have the values of C_{in}, C_o, L , for predefined values of ξ and ω_0 ; that is to say the dimensioning of the *DC/DC* converters to have predefined performances in the dynamic responses. So if we apply the equation (27) on the transfer functions in (18) (19) (20), we obtain the formula of ξ and ω_0 for the different topologies shown in table 2:

Table 2. Analytical forms of (ξ) and (ω_0) for different converters topologies.		
Converter topology	Damping coefficient ξ	Natural pulsation ω_0
buck	$\frac{C_{in} \cdot (L + C_{in} \cdot R_{pv}^2)(1-d)^2 + LC_o(1-d)^2 + (C_o R_{pv})^2}{2R_{pv}(1-d)\sqrt{2L(C_{in}(1-d)^2 + C_o)^3}}$	$\sqrt{\frac{2(1-d)^2}{L(C_{in}(1-d)^2 + C_o)}}$
boost	$\frac{C_o^2 R_{pv}^2 d^6 + (C_{in}^2 R_{pv}^2 + LC_o)d^2 + LC_{in}}{2R_{pv}d(1-d)\sqrt{2L(C_{in}(1-d)^2 + C_o d^2)^3}}$	$\sqrt{\frac{2d^2}{L(C_{in} + C_o d^2)}}$
Buck-boost	$\frac{(C_o R_{pv} d^3)^2 + C_{in}(L + C_{in} R_{pv}^2 d^2)(1-d)^4 + C_o L d^2 (1-d)^2}{2R_{pv}d(1-d)\sqrt{2L(C_{in}(1-d)^2 + C_o d^2)^3}}$	$\sqrt{\frac{2d(1-d)^2}{L(C_{in}(1-d)^2 + C_o d^2)}}$

With the same approach, we expand the equation (22) to get the new coefficients of the nominator ($N_r, N'_1,$

N'_2) as a function of N_2, N_1, N_0 and s_r , so:

$$N_r = N_2 - \left(\frac{N_1}{s_r}\right) - \left(\frac{N_0}{s_r^2}\right) \quad (28)$$

$$N'_1 = -\left(\frac{N_1}{s_r}\right) - \left(\frac{N_0}{s_r^2}\right) \quad (29)$$

$$N'_2 = -2\xi\omega_0 N_2 - \left(\frac{N_0}{s_r}\right) \quad (30)$$

The system of equation (27) with equations (28), (29), (30) models an open loop transfer function of a second order system, whose input is the duty cycle (d), and the output is the voltage (V_{pv}), the dynamic response depends entirely on the damping coefficient (ξ) and the natural pulsation (ω_0), that offers us the exact dimensioning of our circuit by a coherent choice of the elements (C_{in}, C_o, L).

3.3. Closed loop transfer function.

In the previous section, we obtained an open loop transfer function, it models the *DC/DC* transformer shown in figure (2) brings back to the primary without feedback [16], but the MPPT control, associated with a *DC/DC* converter, makes to operate the photovoltaic generator so as to permanently produce the maximum of its power. This specific command must cause the electrical source (solar panel) to operate at the maximum points of their characteristics without these points being known in advance, nor knowing when they were modified; for this, a feedback is provided by a permanent measurement of the power delivered by the photovoltaic generator (I_{pv}, V_{pv}), this measurement is processed by the MPPT block and modulated in the PWM command to have a duty cycle (D) which gives an operating point of maximum power. Figure 5.

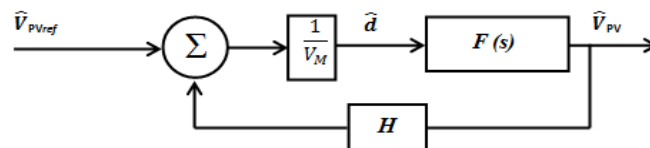


Figure 5. The closed loop model of the *DC/DC* converter controlled by MPPT and PWM command.

(\hat{V}_{PV-ref}) is the reference voltage calculated by the MPPT block, which gives a maximum operating point, this voltage is compared all the time with the real value of the panel voltage (V_{PV}); the resulting value is compared with a triangular signal of amplitude V_M . Figure 6.

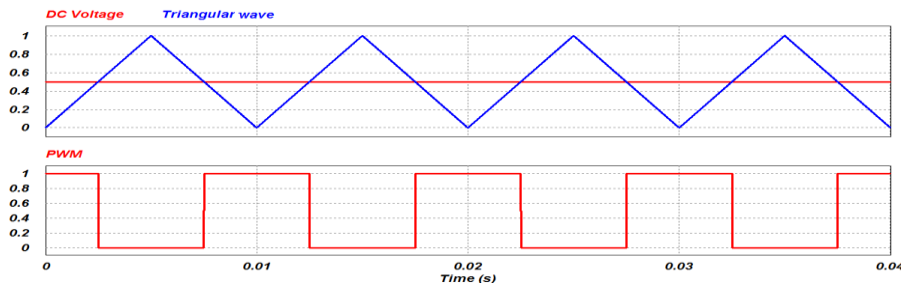


Figure 6. The PWM Signal.

The closed loop the figure 5 in fractional form, nominator of closed loop $N(s)_{cl}$ by the denominator of closed loop $D(s)_{cl}$ is given by:

$$\frac{V_{PV}(s)}{V_{PV,ref}(s)} = \frac{[1/V_M] \cdot F(s)}{1 + [H/V_M] \cdot F(s)} = \frac{N_{cl}(s)}{D_{cl}(s)} \quad (31)$$

Similar to open loop placement, and to have a second order dominating system, the following conditions must be applied:

$$\begin{cases} D_{cl}(s) = 0 \\ |\xi_{cl}| < 1 \\ |s_{r_{cl}}| \gg |\xi \omega_{0_{cl}}| \end{cases} \quad (32)$$

The solution of the system of equation above is, the real pole ($s_{r_{cl}}$), the coefficient of damping (ξ_{cl}) and the natural pulsation $\omega_{0_{cl}}$ according to the coefficients of the polynomial $N_{cl}(s)$ and $D_{cl}(s)$ in a closed loop, therefore the polynomial characteristic $D_{cl}(s)$ is defined as:

$$V_M \cdot s^3 + (N_2 \cdot H + D_2 \cdot V_M) \cdot s^2 + (N_1 \cdot H + D_1 \cdot V_M) \cdot s + (N_0 \cdot H + D_0 \cdot V_M) = 0 \quad (33)$$

Corresponding to the equation (31):

$$D_{3cl} = V_M, D_{2cl} = (N_2 \cdot H + D_2 \cdot V_M), D_{1cl} = (N_1 \cdot H + D_1 \cdot V_M), D_{0cl} = (N_0 \cdot H + D_0 \cdot V_M).$$

The solution is defined as:

$$\begin{cases} s_{r_{cl}} = -D_{2cl} \\ \omega_{0_{cl}} = \sqrt{\frac{D_{0cl}}{D_{2cl}}} \\ \xi_{cl} = \frac{1}{2} \left[\frac{D_{1cl}}{\sqrt{D_{0cl} \cdot D_{2cl}}} - \frac{\sqrt{D_{0cl}}}{D_{2cl} \cdot \sqrt{D_{2cl}}} \right] \end{cases} \quad (34)$$

We can give ξ_{cl} according to the $\omega_{0_{cl}}$ and $s_{r_{cl}}$

$$\xi_{cl} = -\frac{1}{2 \cdot s_{r_{cl}}} \left[\frac{D_{cl1} - \omega_{0_{cl}}^2}{\omega_{0_{cl}}} \right] \quad (35)$$

4. SIZING ALGORITHM.

In previous sections, we have developed equations by the small average signal model of the different DC/DC converter topologies; the objective is to have a transient response similar to a second-order system by the optimal placement of the poles. From different equations; we can observe that:

- The poles are a function of a passive elements of the DC/DC converter circuit (L, C_{in}, C_o), and the amplitude of the carrier of the PWM signal (V_M) and the measurement gain H . All these elements are

fixed a priori during the implementation of the circuit. The values of these poles will decide the stability margin of the system and the transient behavior.

- The poles are a function of (R_{PV}) a resistance that characterizes the maximum operating point. It is highly fluctuating depending on weather conditions (temperature and lighting). Therefore, the choice of the elements (L, C_{in}, C_o), must satisfy the conditions imposed on the transient answer whatever the interval variation of the R_{PV} .
- These poles are also depending on duty cycle (d) calculated by MPPT order must be robust against an interval variation. The study of the three poles as a function of the duty cycle (d) is necessary for a better placement of poles (i.e. the system always remains a second order whatever the variations of (d)). Also for the changes of (R_{PV}); the system response must always have a desired transient, (a damped response and a short response time; a considerate choice of elements (L, C_{in}, C_o, V_M, H) which gives (ξ, ω_0) constant over a large range of variation of (d) will be the best. In our approach, the small average signal model allows us to have the factors of the transfer functions open loop and closed loop, the good dimensioning of these factors (dominant second order system) gives the best values of the various elements of the converters under any topology (buck, boost, and buck-boost), and the good response under any conditions; the proposed algorithm, is designed to make a reliable comparison between the three topologies, for the choice of the best converter which gives a short and well damped transient state.

The procedure for sizing our circuit begins with the calculation of the values of (L, C_{in}, C_o) which gives the continuous condition (CCM), the second step is to have the linear model with the method of the small signal model, this gives the possibility of having the transfer function in the form nominator on the denominator, in the third step the negative discriminator of the polynomial characteristic of the denominator imposes three solutions, one of which is real and the other two are complex conjugates, this gives us the possibility of imposing a second order system by a placement of the poles whose real pole will be the largest possible, at the end the position of the two conjugate poles gives the desired transient response, during all these steps the calculation of the different elements (L, C_{in}, C_o, V_M, H) must be updated to ensure all conditions in open loop or in feedback.

The different steps developed and explained above can be summarized in the following algorithm:

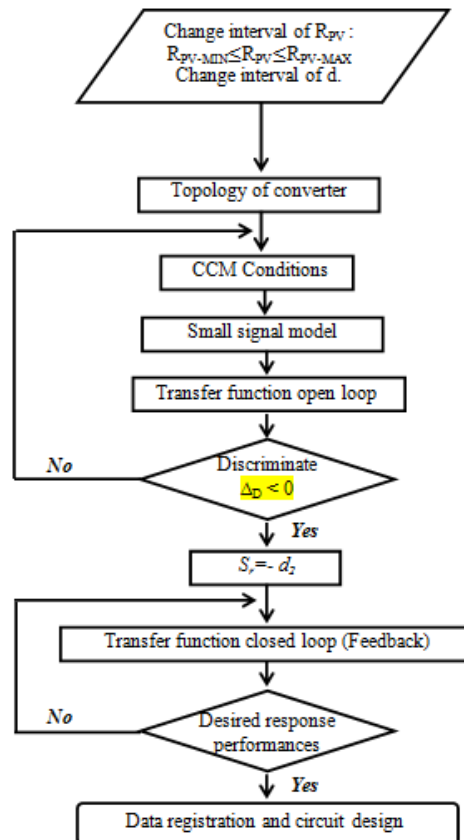


Figure 6. Sizing algorithm for a dynamic response similar to a second order system.

5. SIMULATION RESULTS AND DISCUSSION

For the test of our development approach, we opted for a solar generator which gives under standard conditions (an illumination of 1000 W/m^2 , under a temperature of 25 C°) a voltage $V_{pv}=21 \text{ (V)}$ and current $I_{pv}=7\text{(A)}$; which corresponds to a resistance $R_{pv}=3 \text{ (\Omega)}$, the measurement gain $H=0.01$, and the maximum carrier voltage of the PWM command $V_M=1\text{(V)}$, and the values, $C_{in}=700 \text{ uF}$ $C_0=900 \text{ uF}$ and $L=15\text{mH}$; Gives continuous conduction mode for the three topologies. According to the algorithm above, the first step is to ensure that the discriminant of the denominator of the transfer function is strictly negative, the discriminating curve for the three topologies as a function of the R_{pv} , and duty cycle (d) is represented in the figure 8 and figure 11. In this first step, the circuit elements are chosen to have a negative discriminant whatever the values of the duty cycle (d) and R_{pv} .

in figures 9 and 10, the plot of the damping coefficient and the pulsation as a function of (d) and (R_{pv}), gives us the best interval for a well-damped and short transient time, the boost converter gives better results by a damping coefficient less than 1 for R_{pv} less than 6 (Ω), the boost pulsation is constant ($\omega=220 \text{ rad/s}$), whatever the value of R_{pv} . In figures 12 and 13, we plotted the same curve, but according to the duty cycle (d). For the boost converter, the damping coefficient is less than 1 for (d) less than 0.7, and the pulsation decreases slightly. In figures 15 and 17, we can see the effect of the placement of the poles on the transient state, for a boost converter we have a response time (0.035 s) compared to (0.08 s) for a buck converter which always gives an advantage for the boost converter. For the buck-boost converter, figure 18 and figure 19 the dominant system obtained with the same values of the (L, C_{in}, C_0, V_M, H) is a first order system with a response time of 0.046 s and an overshoot of 65%. These results of the buck-boost converter require recalculation of the values chosen before, to properly compare the three topologies. From the simulation results, we see an advantage of the boost converter.

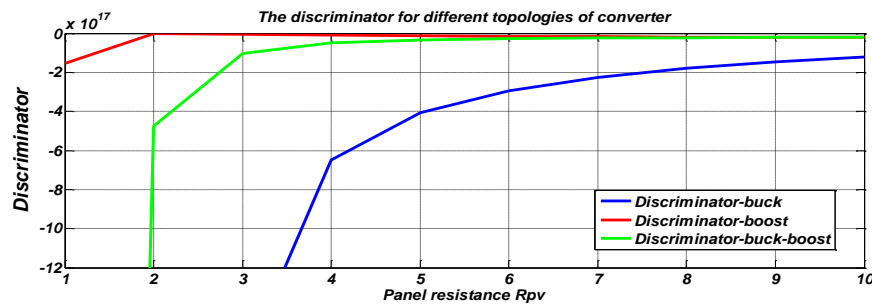


Figure 8. The discriminator according to R_{pv} for the different topologies ($d=0.5$).

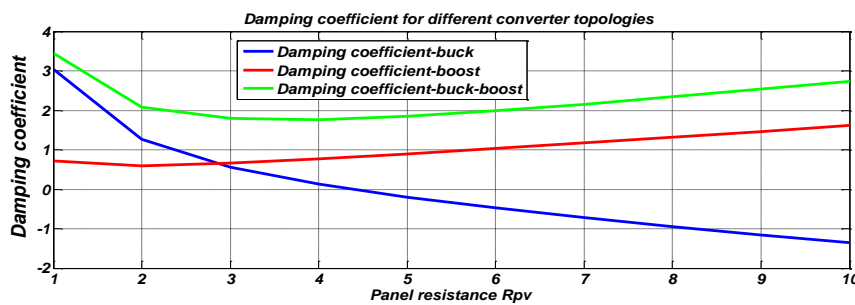


Figure 9. The damping coefficient according to R_{pv} for the different topologies ($d=0.5$).

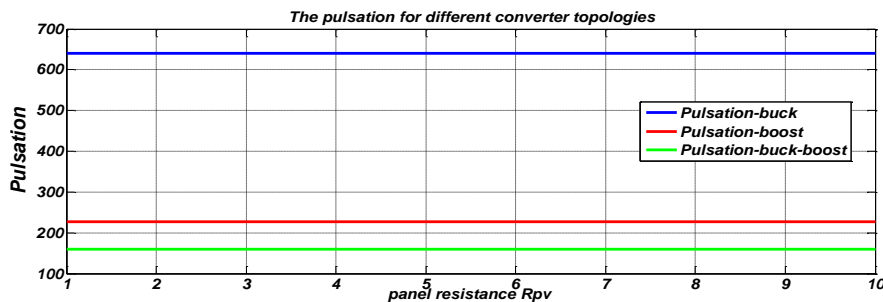


Figure 10. The pulsation according to R_{pv} for the different topologies ($d=0.5$).

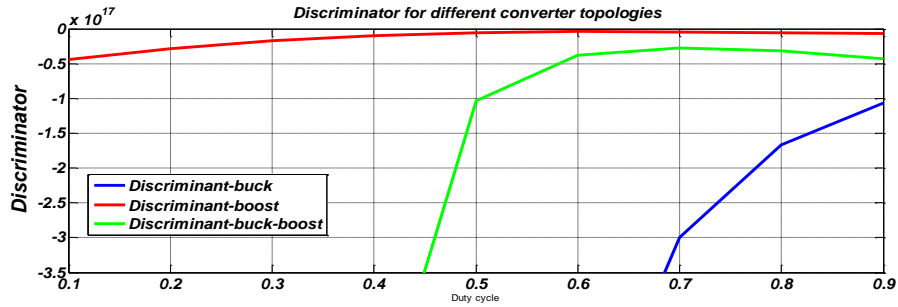


Figure 11. The discriminator according to d for the different topologies ($R_{pv}=3\Omega$).

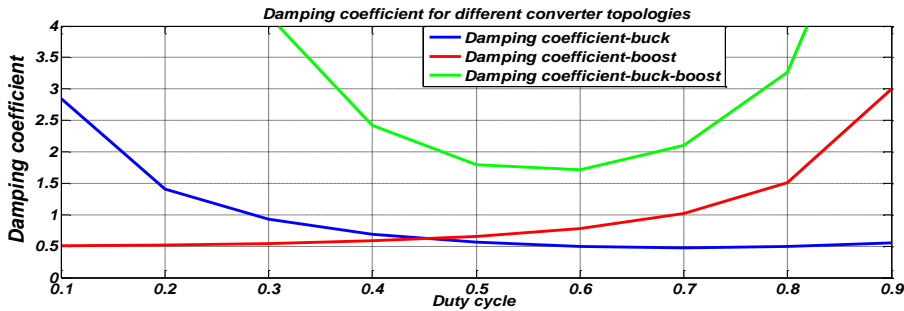


Figure 12. The damping coefficient according to d for the different topologies ($R_{pv}=3\Omega$).

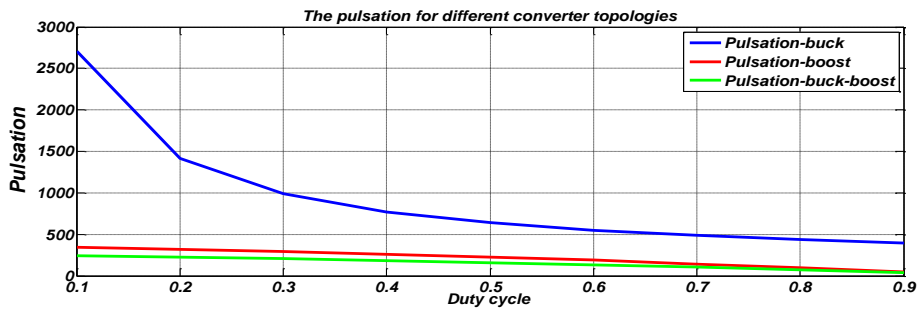


Figure 13. The pulsation according to d for the different topologies ($R_{pv}=3\Omega$).

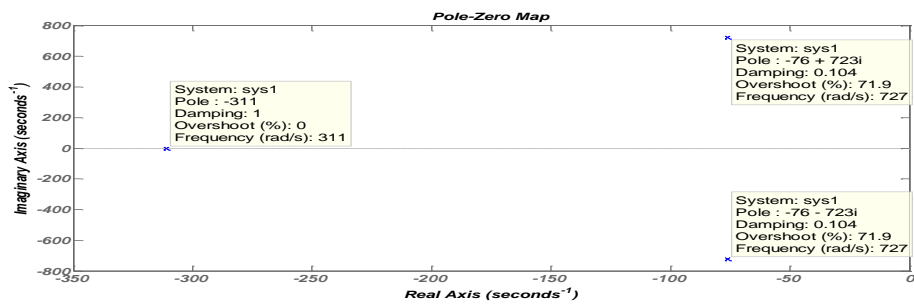


Figure 14. The placement of the poles for the buck topology ($R_{pv}=3\Omega$, $d=0.5$).

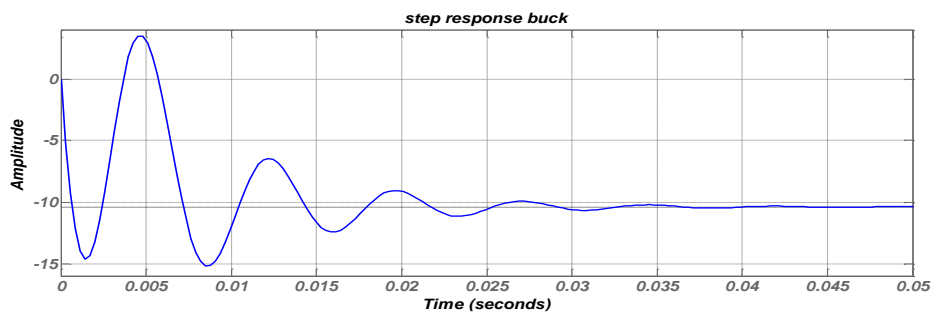


Figure 15. The step reponse for the buck topology ($R_{pv}=3\Omega$, $d=0.5$).

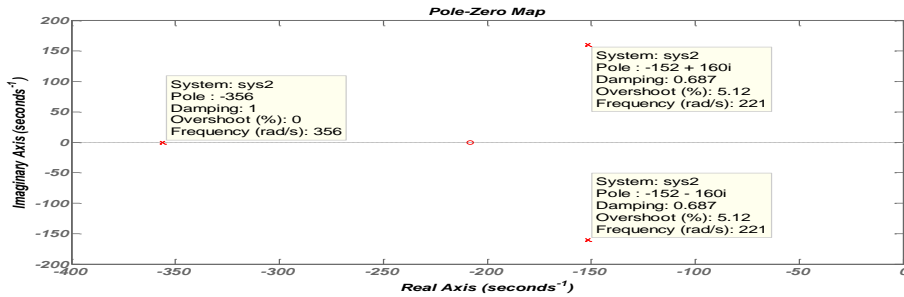


Figure 16. The placement of the poles for boost topologie ($R_{pv}=3\Omega$, $d=0.5$).

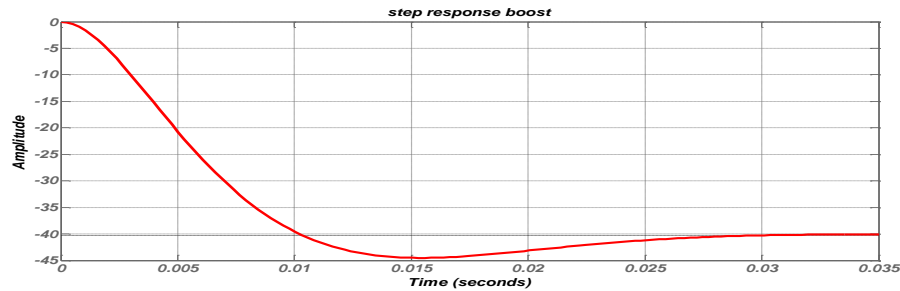


Figure 17. The step reponse of the boost topologie ($R_{pv}=3\Omega$, $d=0.5$).

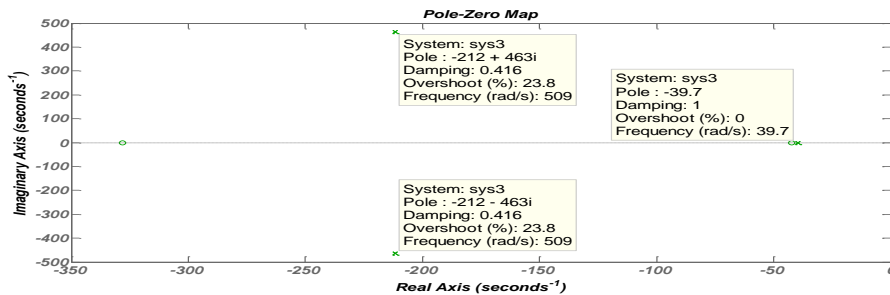


Figure 18. The placement of the poles for the buck-boost topologie ($R_{pv}=3\Omega$, $d=0.5$).

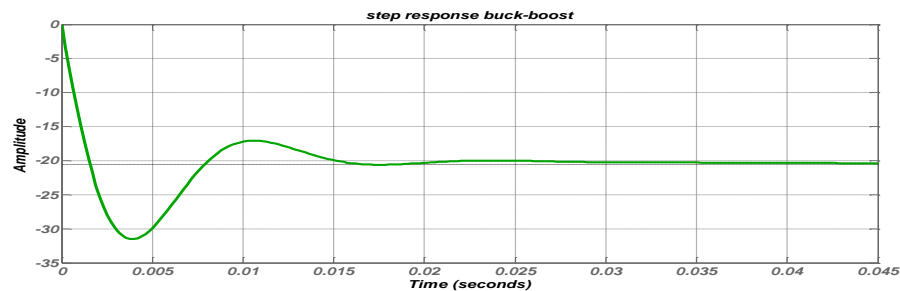


Figure 19. The step reponse for the buck-boost topologie ($R_{pv}=3\Omega$, $d=0.5$).

The method of designing the *DC/DC* converters by the algorithm presented above, has the advantage of having a desired dynamic response whatever the fluctuations caused by meteorological changes (lighting and temperature), in addition, we can past the use of the PI corrector which often requires complicated adjustment (compared to articles [7] and [8]), the calculation of the proportional and integral gains (K_p , K_i) remains until now a challenge for the researchers, it amounts to the difficulty of determining these two gains to have the desired dynamics in a large interval variation, one often uses the logic fuzzy and neural networks to calculate these two gains; Unfortunately, these methods have a high computational cost ; in addition, it is known that the speed and the precision are inversely proportional in this kind of design. In addition, always in [7], the use of a PI corrector can destabilize the system if the inputs are not appropriate. On the other hand, in the articles [4], the author does not use the PI corrector, and he bases his optimization on the parameters of the MPPT (the amplitude of the disturbance and the sampling step), the paper does not give any indication on the

choice of circuit elements during a change in lighting and temperature, although these optimization parameters developed in the theoretical study are a function of the resistance R_{pv} and the duty cycle d . With our approach proposed in this article, we can avoid the adjustment of the sampling step which only limits the optimization with digitally implanted MPPTs. The results quoted above also give us the advantage of making a technical and economic comparison between the three topologies of DC/DC converters, to ensure a better choice according to predefined specifications. The best DC/DC converter is one that provides a fast, well-damped response time over a wide range of R_{pv} and d , and ensures stability and accuracy regardless of change. From an economic point of view, the best converter will be the one that guarantees the aforementioned technical characteristics at the lowest possible cost (the minimum values of C_{in} , C_o , L , H , and VM). The chosen topology gives us the best procedure when using DC/DC converters in photovoltaic applications, either increase the voltage (the boost use), lower the voltage (the buck use), or increase/lower the voltage (using buck/boost).

6. CONCLUSION

In this paper, a dimensioning method has been developed for an optimal design of the conventional DC/DC converters used in MPPT. By the small signal average model we establish linear transfer functions for the three topologies of the DC/DC converters, a second order system is obtained by placing dominant poles; the study of the different factors such as the natural frequency and the damping coefficient can give us the best design of the DC/DC converters which gives a better transitory response and improved dynamic of the system under different conditions (variation of illumination and temperature). In perspective, we will use the methods of operations research to make a deeper technical-economic comparison between the different types of converter topologies and tested our algorithm by an experimental implementation.

REFERENCES

- [1] S. Gorjina, A. Shukla, *Photovoltaic Solair Energy Conversion, Technologies, Applications and Environmental Impacts*, Academic Press, imprint of Elsevier 125 London Wall, London EC2Y 5AS, United Kingdom, 2020.
- [2] Y. Yang, K. A. Kim, F. Blaabjerg, A. Sangwongwanich, *Advances in Grid-Connected Photovoltaic Power Conversion Systems*, Woodhead Publishing, imprint of Elsevier Mess Business Centre, Royston Road, Duxford, CB22 4QH, United Kingdom, 2019.
- [3] G. Petron, C. Andrés Ramos-Paja, G. Spagnuolo, *Photovoltaic Sources Modeling*, 1rd ed. John Wiley-IEEE PRESS, 2017.
- [4] N. Femia, G. Petron, G. Spagnuolo, M. Vitelli, *Power Electronics and Control Techniques for Maximum Energy Harvesting in Photovoltaic Systems*, 1rd ed. CRC Press Taylor & Francis Group 6000 Broken Sound Parkway NW, 2013.
- [5] N. Femia, G. Petrone, G. Spagnuolo, and M. Vitelli, "Optimization of Perturb and Observe Maximum Power Point Tracking Method," *IEEE Transactions on power electronics*, Vol. 20, No. 4, July 2005.
- [6] J. N. Hemalatha, S. A. Hariprasad, G. S. Anitha, "Control Strategy to Generate PWM Signals with Stability Analysis for Dual Input Power Converter System," *Indonesian Journal of Electrical Engineering and Informatics (IJEEI)*, Vol. 7, No. 4, Dec 2019, pp. 609~619.
- [7] R. Ayop, C. Wei Tan, K. Yiew Lau, "Computation of current-resistance photovoltaic model using reverse triangular number for photovoltaic emulator application," *Indonesian Journal of Electrical Engineering and Informatics (IJEEI)*, Vol. 7, No. 2, June 2019, pp. 314~322.
- [8] H. A. Ismail, A. Alenany, and B. Abozalam, "Improved DC-Link Voltage Controller for Photo Voltaic ON-Grid Systems," *Indonesian Journal of Electrical Engineering and Informatics (IJEEI)*, Vol. 9, No. 2, June 2021, pp. 442~452.
- [9] H. Snani, M. Amarouayache, A. Bouzid, A. Iashab and H. Bounechba, "A Study of Dynamic Behaviour Performance of DC/DC Boost Converter used in the Photovoltaic System" *Proceedings 15th IEEE International Conference on Environment and Electrical Engineering*, pp. 1966 – 1971, 2015.
- [10] [2] H. snani, M. Amrouayache, A. Bouzid, "Dynamic behavior overview of three conventional dc/dc converters used in PV MPPT system" *Revue des Energies Renouvelables* Vol. 20 N°2 (2017) 319 – 333.
- [11] Efstratios I. Batzelis, G. Anagnostou, Ian R. Cole, Thomas R. Betts, and Bikash C. Pal, "A State-Space Dynamic Model for Photovoltaic Systems With Full Ancillary Services Support," *IEEE Transaction in sustainibale energy*, Vol. 10, No. 3, July 2019.
- [12] Y. Rudenko, "Analysis of DC-DC Converters by Averaging Method based on Lagrange Theorems," *2021 IEEE 2nd KhPI Week on Advanced Technology (KhPIWeek)*.
- [13] A. Raj, R.P. Praveen, "Highly efficient DC-DC boost converter implemented with improved MPPT algorithm for utility level photovoltaic applications," *Ain Shams Engineering Journal (journal 13) 2022*, Production and hosting by Elsevier.
- [14] W. Xiao, N. Ozog, and William G. Dunford, "Topology Study of Photovoltaic Interface for Maximum Power Point Tracking," *IEEE Transactions on industrial electronics*, Vol. 54, No. 3, June 2007.
- [15] Efstratios I. Batzelis *et al.*, "A State-Space Representation of Irradiance-Driven Dynamics in Two-Stage Photovoltaic Systems," *IEEE Journal of Photovoltaics*, Vol 8, No 4, July 2018.

- [16] H. Mishra, S. Ray, "Comprehensive Small Signal Modeling of the DC/DC Converters with CDM Controller Design," *2020 First International Conference on Power, Control and Computing Technologies (ICPC2T)*, 2020.
- [17] R. W. Erickson and D. Maksimovic', *Fundamental of Power Electronics*. Norwell, 2nd ed. MA: Kluwer, 2003.
- [18] S. Neumark, *Solution of Cubic and Quartic Equations*, Elsevier Ltd, Pergamon Press, Oxford, London, Edinburgh, New York, Paris, Frankfurt, 1965.

BIOGRAPHY OF AUTHOR



Amrouayache Mohamed. He was born in Constantine, Algeria in 1976; he obtained his degree in electrical engineering in 2002, Magister in 2006, and his doctoral degree in 2014, from the university of Constantine 1. From 2011 until 2014 he was a researcher at the Center for the Development of Renewable Energies (CDER), Algiers. From 2016, he is a lecturer at the university of Skikda, Algeria. His researches interested at power electronics systems, renewable energies, integrate the renewable energies in electrical networks, and smart grid.